Journal of Medicinal Chemistry

ARTICLE

pubs.acs.org/jmc

Novel ^{18}F-Labeled Benzofuran Derivatives with Improved Properties for Positron Emission Tomography (PET) Imaging of β-Amyloid Plaques in Alzheimer's Brains

Masahiro Ono,*,† Yan Cheng,† Hiroyuki Kimura,† Mengchao Cui,† Shinya Kagawa,‡ Ryuichi Nishii,‡ and Hideo Saji*,†

†Graduate School of Pharmaceutical Sciences, Kyoto University, 46-29 Yoshida Shimoadachi-cho, Sakyo-ku, Kyoto 606-8501, Japan

‡Shiga Medical Center Research Institute, 5-4-30, Moriyama, Moriyama City, Shiga 524-8524, Japan

Supporting Information

ABSTRACT: In vivo imaging of β-amyloid plaques in the brain may lead to the early diagnosis of Alzheimer's disease (AD) and monitoring of the progression and effectiveness of treatment. In the present study, we report on the development of two potential PET probes, [^{18}F]FPYBF-2 ([^{18}F]**10**) and [^{18}F]FPHBF-2 ([^{18}F]**21**), for imaging of β-amyloid plaques in AD brain. In experiments in vitro, **10** and **21** displayed high affinity for Aβ(1−42) aggregates (K_i = 2.41 and 3.85 nM, respectively). In biodistribution experiments using normal mice, they displayed high uptake in the brain (7.38 and 8.18% ID/g at 2 min postinjection, respectively), and the radioactivity washed out from the brain rapidly (3.15 and 3.87% ID/g at 60 min postinjection, respectively), which is highly desirable for β-amyloid imaging agents. In vivo, they clearly labeled β-amyloid plaques in Tg2576 mice. Furthermore, the specific labeling of β-amyloid plaques by **10** and **21** was observed in autoradiographs of sections of autopsied AD brain. These new fluorinated benzofuran derivatives are promising PET probes for imaging cerebral β-amyloid plaques.

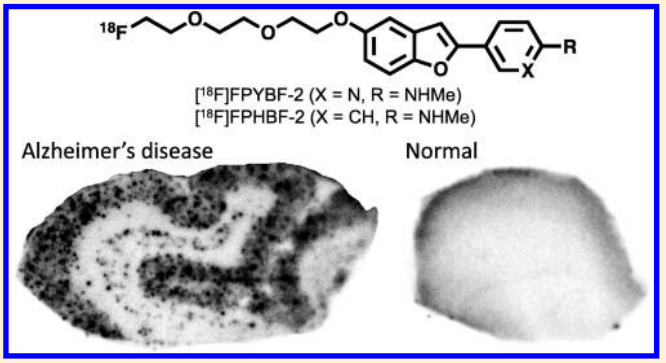

INTRODUCTION

Alzheimer's disease (AD), the most common senile dementia, is characterized by β-amyloid (Aβ) plaques, vascular amyloid, neurofibrillary tangles, and progressive neurodegeneration. The formation of Aβ plaques, composed of Aβ peptides, in the brain is generally accepted as the initial neurodegenerative event in AD.[1,2] The in vivo detection of Aβ plaques in AD brains by positron emission tomography (PET) should be useful for early diagnosis and the discovery of effective therapeutic agents for AD.[3−5]

Initial studies with PET suggested that [^{11}C]4-*N*-methylamino-4′-hydroxystilbene (SB-13),[6,7] [^{11}C]2-(4′-(methylamino phenyl)-6-hydroxybenzothiazole (PIB),[8,9] [^{11}C]2-(2-[2-dimethylaminothiazol-5-yl]ethenyl)-6-(2-[fluoro]ethoxy)benzoxazole (BF-227),[10] and [^{11}C]-2-[6-(methylamino)pyridin-3-yl]-1,3-benzothiazol-6-ol (AZD2184),[11,12] differed in their uptake and retention in the brain between AD patients and controls (Figure 1). Among them, PIB is the best characterized PET imaging agent for Aβ plaques in the brain. In the past few years, successful imaging with PIB in thousands of AD patients has been reported. The utility of PIB to image Aβ plaques in the brain has provided considerable impetus for further refinement of this technique. However, the practical challenges of using PIB labeled with ^{11}C ($t_{1/2}$ = 20 min) on a routine basis have limited its potential as a diagnostic tool. Since additional tracers labeled with ^{18}F with longer half-life ($t_{1/2}$ = 110 min) may be more useful as PET imaging agents for detection and quantification of Aβ plaques, recent efforts have focused on the development of comparable agents labeled with ^{18}F. Previous studies with [^{18}F]2-(1-(2-(*N*-(2-fluoroethyl)-*N*-methylamino)naphthalene-6-yl)ethylidene)malononitrile (FDDNP)[13,14] showed differential uptake and retention in the brain of AD patients for the first time. PET imaging studies in humans suggest that FDDNP shows a higher retention in regions of the brain suspected of having neurofibrillary tangles and Aβ plaques, indicating that it is not for selectively measuring Aβ plaques in AD brains. More recently, a PIB analogue, 2-(3-[^{18}F]fluoro-4-methyaminophenyl)benzothiazol-6-ol (GE-067, flutemetamol),[15−17] a stilbene derivative, (*E*)-4-(*N*-methylamino)-4′-(2-(2-(2-[^{18}F]fluoroethoxy)ethoxy)ethoxy)stilbene (BAY94-9172, florbetaben) ,[18−20] and a styrylpyridine derivative, (*E*)-4-(2-(6-(2-(2-(2-(-[^{18}F]fluoroethoxy)ethoxy)ethoxy)pyridyn-3-ylvinyl)-*N*-methylbenzenamine (AV-45, florbetapir),[21−27] and have been shown to

Received: January 20, 2011
Published: March 23, 2011

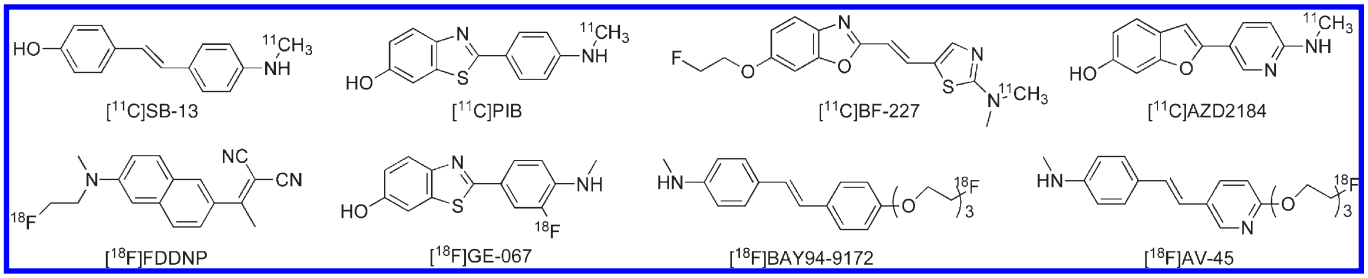

Figure 1. Chemical structures of PET imaging agents targeting β-amyloid plaques in AD patients.

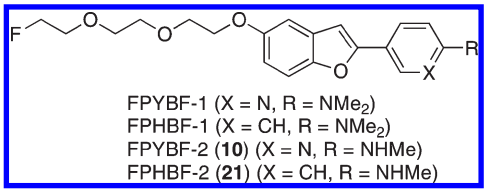

Figure 2. Chemical structure of ^{18}F-labeled benzofuran derivatives reported in the present study.

be useful for the imaging of Aβ plaques in living brain tissue in phase II or III clinical trials (Figure 1).

In the search for PET imaging agents with improved properties, we have recently reported a series of fluorinated benzofuran derivatives as potential ^{18}F-labeled tracers for the imaging of Aβ plaques by PET. First, on the basis of our previous research regarding radioiodinated and ^{11}C-labeled benzofuran derivatives,[28,29] we developed 4-(5-(2-(2-(2-fluoroethoxy)-ethoxy)ethoxy)benzofuran-2-yl)-*N*,*N*-dimethylbenzenamine (FPHBF-1, Figure 2) with a fluoropolyethylene glycol side chain and a dimethyaminophenyl group.[30] Although the penetration of brain tissues by this tracer was encouraging, the slow washout of this probe from the normal mouse brain made it unsuitable for imaging in vivo. Therefore, a critical need to fine-tune the kinetics of the uptake and washout of benzofuran derivatives existed. Previous results regarding uptake into and clearance from the brain point to high lipophilicity as one of the reasons for a slow washout from the brain.[8,29,31,32]

To further improve the pharmacokinetics of the radioactivity in the brain, we planned to develop a novel fluorinated pyridylbenzofuran derivative with less lipophilicity by displacing the phenyl group in phenylbenzofuran with a pyridyl group. Then we designed and synthesized 5-(5-(2-(2-(2-fluoroethoxy)ethoxy)ethoxy)benzofuran-2-yl)-*N*,*N*-dimethylpyridin-2-amine (FPYBF-1, Figure 2) with a fluoropolyethylene glycol side chain and a dimethylaminopyridyl group.[33] This tracer displayed faster clearance from the normal mouse brain than FPHBF-1, without a decrease in uptake and reduction in affinity for Aβ plaques. These results suggested that the pharmacokinetics were improved by reducing the lipophilicity of the benzofuran derivative. While ^{18}F-labeled AV-19 ((*E*)-2-(2-(2-(2-fluoroethoxy)ethoxy)ethoxy)-5-(4-dimethylaminostyryl)pyridine) showed promising results in animal studies, its uptake in humans was lower than expected possibly because of a rapid metabolism of its dimethylamino group.[27] However, monomethylation of AV-19 led to the formation of AV-45, which exhibited excellent uptake and washout in the brain in humans.[22,27] Furthermore, all PET imaging probes in phase III clinical trials (AV-45, BAY94-9172, and GE067, Figure 1) have a monomethylamino group that is stable in vivo and reduces the lipophilicity of the compounds compared with a dimethylamino group.

In the present study, we designed and synthesized novel fluorinated pyridylbenzofuran and phenylbenzofuran derivatives (FPYBF-2 and FPHBF-2, Figure 2) with a fluoropolyethylene glycol side chain and a monomethylamino group. We here report the synthesis and biological evaluation of two new ^{18}F benzofuran derivatives with a monomethylamino group in comparison with the corresponding benzofuran derivatives with a dimethylamino group.

RESULTS AND DISCUSSION

The synthesis of FPYBF-2 (**10**) and FPHBF-2 (**21**) is outlined in Schemes 1 and 2, respectively. The key step in the formation of the fluorinated pyridylbenzofuran backbone is accomplished by Suzuki coupling between 5-methoxybenzofuran-2-boronic acid and 2-amino-5-iodopyridine.[34] Suzuki coupling afforded the desired compound **1** in a yield of 52%. The key step in the formation of the phenylbenzofuran backbone was readily achieved by reacting 2-hydroxy-5-methoxybenzaldehyde with 4-nitrobenzyl bromide to produce **11** in a yield of 64%. The amino derivative **12** was prepared from **11** by reduction with $SnCl_2$ in a yield of 49%. Conversion of **1** and **12** to the monomethylamino derivatives **2** and **13** was achieved by the monomethylation of the amino group by using a method[29] previously reported in yields of 92% and 95%, respectively. A methoxy group of **2** and **13** was converted to a hydroxyl group using BBr_3/CH_2Cl_2, which afforded **3** and **14** in yields of 99 and 99%, respectively. To prepare compounds with three ethoxy groups as the polyethylene glycol linkage, 2-[2-(2-chloroethoxy)ethoxy]ethanol was coupled with the OH group of **3** and **14** to obtain **4** and **15**. The free OH groups of **4** and **15** were subsequently protected with *tert*-butyldimethylsilyl chloride (TBDMSCl) to give **5** and **16**. Compounds **6** and **17** were obtained by protecting the methylamino groups of **5** and **16**. After removal of the TBS-protected groups of **5** and **16** with tetrabutylammonium fluoride (TBAF) in tetrahydrofuran (THF), the free OH groups of **7** and **18** were converted into mesylates by reacting with MsCl in the presence of triethylamine to give **8** and **19**. The fluorinated benzofuran derivatives **10** and **21** were successfully obtained by refluxing **8** and **19** in anhydrous TBAF/THF followed by stirring with TFA to remove the butyloxycarbonyl (BOC) protected group.

To prepare the desired ^{18}F-labeled benzofuran derivatives, the *N*-BOC-protected mesylates **8** and **19** were employed as the precursors (Scheme 3). Each of the mesylates was reacted with [^{18}F]fluoride/potassium carbonate and Kryptofix 222 in acetonitrile. The mixture was then treated with aqueous HCl to remove the *N*-BOC-protected group. After purification of the crude product by HPLC, the ^{18}F-labeled **10** ([^{18}F]FPYBF-2) and **21** ([^{18}F]FPHBF-2) were prepared with an average radiochemical

Scheme 1[a]

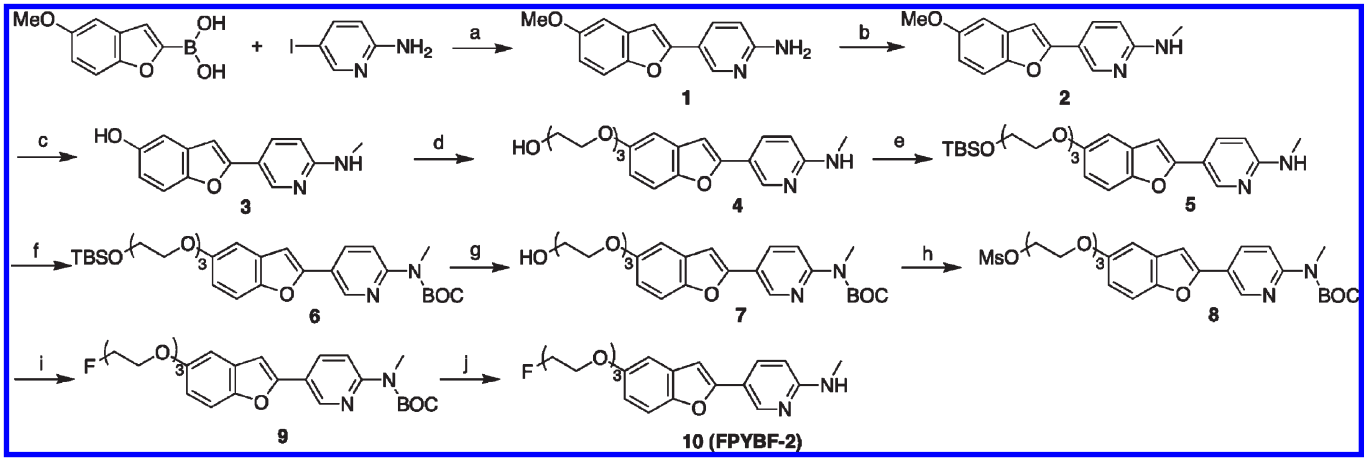

[a] Reagents: (a) $(Ph_3P)_4Pd$, Na_2CO_3(aq)/dioxane; (b) (1) NaOMe, MeOH, $(CH_2O)_n$; (2) $NaBH_4$; (c) BBr_3, CH_2Cl_2; (d) 2-[2-(2-chloroethoxy)ethoxy]ethanol, K_2CO_3, DMF; (e) TBDMSCl, imidazole, CH_2Cl_2; (f) $(BOC)_2O$, THF; (g) TBAF, THF; (h) MsCl, Et_3N, CH_2Cl_2; (i) TBAF, THF; (j) TFA, CH_2Cl_2.

Scheme 2[a]

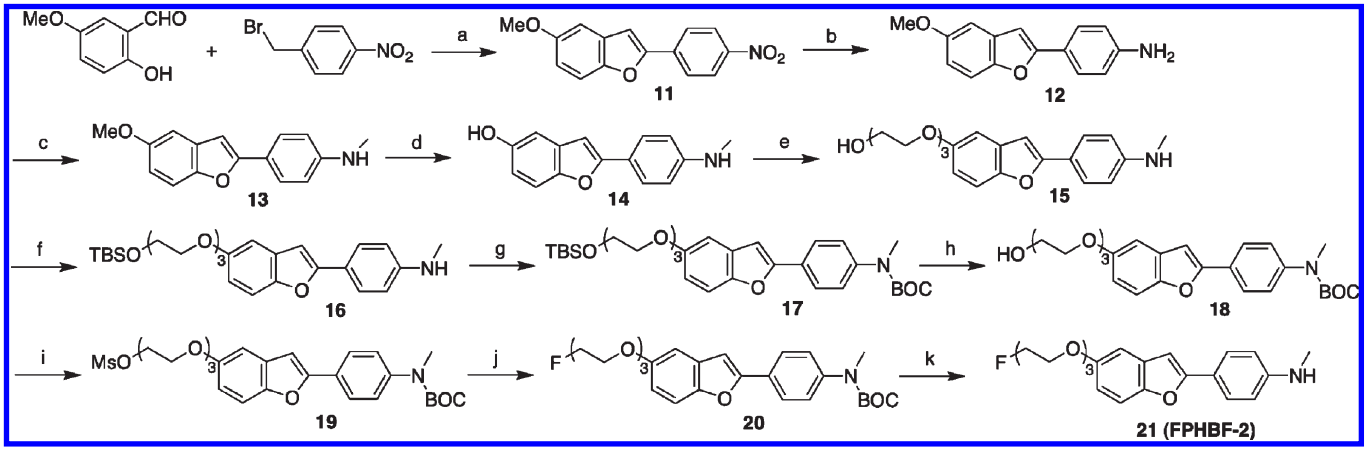

[a] Reagents: (a) K_2CO_3, DMF; (b) $SnCl_2$, EtOH; (c) NaOMe, $(CH_2O)_n$, MeOH; (d) BBr_3, CH_2Cl_2; (e) 2-[2-(2-chloroethoxy)ethoxy]ethanol, K_2CO_3, DMF; (f) TBDMSCl, imidazole, CH_2Cl_2; (g) $(BOC)_2O$, THF; (h) TBAF, THF; (i) MsCl, Et_3N, CH_2Cl_2; (j) TBAF, THF; (k) TFA, CH_2Cl_2.

Scheme 3[a]

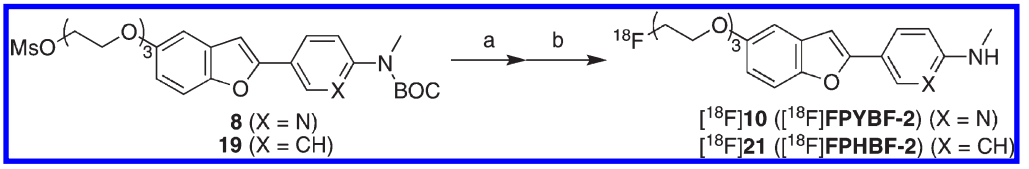

[a] Reagents and conditions: (a) Kryptofix 222/K_2CO_3, $^{18}F^-$, MeCN, 120 °C, 5 min; (b) 10%HCl (aq), 120 °C, 5 min.

yield of 52% and radiochemical purity of >99% and a specific activity of 242 GBq/μmol. The identity of [^{18}F]**10** and [^{18}F]**21** was verified by a comparison of the retention time with that of the nonradioactive compound (see Supporting Information).

Experiments in vitro to evaluate the affinity of the fluorinated benzofuran derivatives for Aβ aggregates were carried out in solutions with [^{125}I]2-(4′-dimethylaminophenyl)-6-iodoimidazo[1,2-*a*]pyridine ([^{125}I]IMPY) as the ligand according to conventional methods.[35,36] Compounds **10** and **21** inhibited the binding of [^{125}I]IMPY with a K_i of 2.41 and 3.85 nM, respectively, indicating that they have excellent affinity for Aβ(1−42) aggregates (Table 1). The *N*-monomethylated derivatives (**10** and **21**) exhibited slightly less affinity (K_i = 2.41 and 3.85 nM, respectively) than the N,N-dimethylated derivatives (FPYBF-1 and FPHBF-1) (0.95 and 2.00 nM, respectively). In addition, **10** and **21** showed higher binding affinity than PIB and IMPY, well-known Aβ imaging probes (K_i = 9.00 and 10.5 nM, respectively), in the same assay. The result suggests that removing the methyl group from a dimethylamino group of FPYBF-1 and FPHBF-1 reduces the affinity for Aβ aggregates. It also indicates that the electronegativity of the nitrogen

dx.doi.org/10.1021/jm200057u |*J. Med. Chem.* 2011, 54, 2971–2979

Table 1. Inhibition Constants of Benzofuran Derivatives on Binding to Aβ42 Aggregates

compd	K_i (nM)[a]	ClogP[b]
10	2.41 ± 0.11	2.32
21	3.85 ± 0.22	2.94
FPYBF-1	0.95 ± 0.21	3.11
FPHBF-1	2.00 ± 0.50	3.73
PIB	9.00 ± 1.31	3.28
IMPY	10.50 ± 1.05	3.79

[a] Values are the mean ± standard error of the mean for three independent experiments. [b] The calculated logarithms of water−octanol partition coefficients (ClogP) were obtained using ChemDraw Ultra 10.0 software (CambridgeSoft, Cambridge, MA).[46]

Table 2. Biodistribution of Radioactivity after Intravenous Administration of ^{18}F-Labeled Benzofuran Derivatives in Mice[a]

	time after injection (min)			
tissue	2	10	30	60
		[^{18}F]**10**		
blood	4.96 (0.38)	3.02 (0.12)	2.66 (0.34)	2.42 (0.13)
brain	7.38 (0.84)	4.86 (0.41)	4.03 (0.61)	3.15 (0.10)
bone	2.65 (0.35)	1.63 (0.13)	1.79 (0.17)	1.72 (0.27)
liver	16.8 (2.20)	17.5 (1.81)	19.2 (2.64)	8.71 (0.99)
kidney	11.9 (0.93)	6.22 (0.66)	7.83 (1.18)	3.70 (1.79)
intestine	4.24 (0.51)	8.39 (2.04)	24.1 (5.76)	30.9 (8.00)
spleen	2.91 (0.42)	2.15 (0.14)	3.14 (0.61)	2.24 (0.35)
lung	5.68 (0.33)	3.12 (0.21)	4.34 (0.77)	2.88 (0.27)
pancreas	5.14 (0.48)	2.68 (0.29)	4.91 (2.21)	2.55 (0.21)
heart	5.19 (0.39)	2.51 (0.28)	3.59 (0.48)	2.60 (0.23)
stomach[b]	3.73 (0.81)	7.55 (2.09)	18.8 (5.69)	22.5 (2.56)
		[^{18}F]**21**		
blood	4.10 (0.56)	4.17 (0.32)	5.33 (0.33)	7.33 (1.01)
brain	8.18 (0.59)	6.43 (0.66)	4.26 (0.42)	3.87 (0.42)
bone	1.57 (0.62)	1.98 (0.16)	2.07 (0.16)	3.30 (0.25)
		[^{18}F]FPYBF-1		
blood	2.83 (0.89)	2.13 (0.49)	1.76 (0.09)	1.98 (0.35)
brain	5.16 (0.30)	3.75 (0.64)	2.78 (0.22)	2.44 (0.36)
bone	1.61 (0.33)	1.33 (0.28)	1.11 (0.13)	1.42 (0.24)
		[^{18}F]FPYBF-1		
blood	1.64 (0.07)	2.48 (0.18)	2.68 (0.26)	3.41 (0.56)
brain	2.88 (0.46)	5.66 (0.31)	3.14 (0.26)	2.80 (0.06)
bone	1.19 (0.18)	1.76 (0.13)	3.63 (1.11)	2.74 (0.59)

[a] Expressed as % injected dose per gram. Each value represents the mean (SD) for five animals at each interval. [b] Expressed as % injected dose per organ.

atom of the aminophenyl group plays an important role in determining binding affinity. A similar change in affinity for Aβ aggregates after *N*-methyl groups were added has been observed for stilbene,[37] styrylpyridine,[38] flavone,[31] chalcone,[39] and aurone[40] derivatives containing a *p*-aminophenyl group.

To evaluate the uptake of [^{18}F]**10** and [^{18}F]**21** in the brain, a biodistribution experiment was performed in normal mice (Table 2).

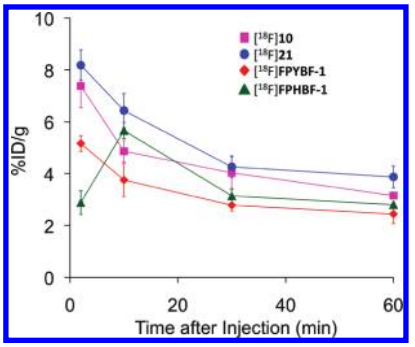

Figure 3. Comparison of brain uptake of four ^{18}F-labeled benzofuran derivatives in normal mice.

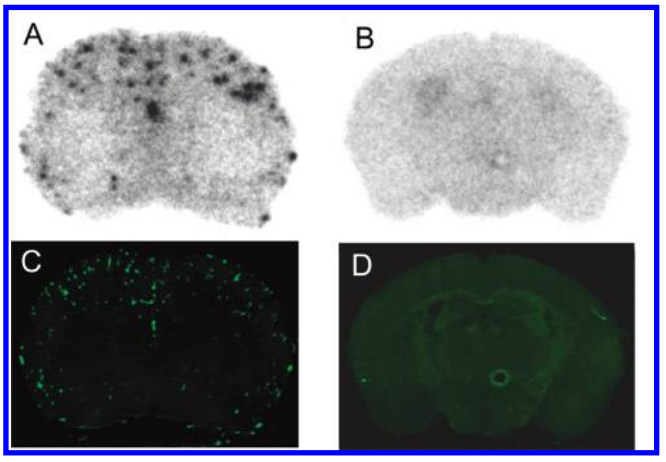

Figure 4. Ex vivo plaque labeling in brain sections from a Tg2576 mouse (A) and a wild-type mouse (B) with [^{18}F]**10**. The same sections were also stained with thioflavin-S (C, D).

[^{18}F]**10** and [^{18}F]**21** displayed high uptake (7.38 and 8.18% ID/g) at 2 min postinjection; these values were comparable to those reported for BAY94-9172 and AV-45, which are under phase III clinical trials. The uptake of [^{18}F]**10** and [^{18}F]**21** was higher than that of [^{18}F]FPYBF-1 and [^{18}F]FPHBF-1 with a dimethylamino group. The radioactivity in the brain after the injection of [^{18}F]**10** and [^{18}F]**21** cleared with time (3.15 and 3.87% ID/g at 60 min postinjection). Since there are no Aβ plaques in the brain of normal mice, a high initial uptake and rapid washout in normal mouse brain are highly desirable properties for Aβ plaque-targeting imaging agents. To directly compare the uptake and washout of four ligands tested in this study, a combined plot is presented in Figure 3. The $\text{brain}_{2\text{min}}/\text{brain}_{60\text{min}}$ ratio as an index to compare the washout rate is used for determining the radioactivity pharmacokinetics in vivo.[40] The $\text{brain}_{2\text{min}}/\text{brain}_{60\text{min}}$ ratio of [^{18}F]**10**, [^{18}F]**21**, [^{18}F]FPYBF-1, and [^{18}F]FPHBF-1 was 2.34, 2.11, 2.11, and 1.02, respectively, indicating that [^{18}F]**10** provided the best profile of radioactivity in the brain among the four ligands. Although the $\text{brain}_{2\text{min}}/\text{brain}_{60\text{min}}$ ratio of [^{18}F]**10** (2.34) was lower than that of [^{18}F]BAY94-9172 (4.8)[18] or [^{18}F]AV-45 (3.8),[21] it was improved compared to values for [^{18}F]FPYBF-1 (2.11) reported previously.[30] The favorable in vivo pharmacokinetics of [^{18}F]**10** were achieved by changing the dimethylaminophenyl group in [^{18}F]FPYBF-1 to a monomethylaminophenyl group. Although lipophilicity is just one of the factors affecting the uptake of a compound into the brain, previous results suggest the lipophilicity of Aβ imaging agents to play an important role in uptake and washout. The results observed for [^{18}F]**10** and

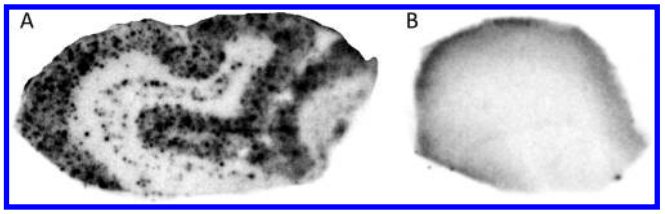

Figure 5. In vitro autoradiograms of sections of AD brain labeled with [^{18}F]**10**. Intensive labeling of β-amyloid plaques in brain tissue from AD patients is shown (A). The control subject exhibits no labeling by this tracer (B).

[^{18}F]**21** suggest that the introduction of further hydrophilic groups into the pyridylbenzofuran and phenylbenzofuran scaffold may lead to the development of more useful pyridylbenzofuran and phenylbenzofuran derivatives. No marked uptake of [^{18}F]**10** and [^{18}F]**21** in the bone was observed (1.72 and 3.30% ID/g, respectively), suggesting little defluorination in vivo, and so interference with the imaging is expected to be relatively minor.

To further characterize the potential of these probes in living brain tissue, we carried out autoradiography ex vivo in Tg2576 mice (36 months, male) and in wild-type mice (36 months, male) as age-matched controls (Figure 4). Tg2576 transgenic mice show marked Aβ deposition in the brain by 11−13 months of age[41] and have been frequently used to evaluate the specific binding of Aβ plaques in experiments in vitro and in vivo.[39,42,43] The autoradiography using [^{18}F]**10** showed distinctive labeling of Aβ plaques in the Tg2576 mouse brain (Figure 4A), while wild-type mouse brain showed no such labeling (Figure 4B). Aβ plaques were confirmed to be present by costaining the sections with thioflavin-S, a dye commonly used to stain Aβ plaques (Figure 4C). When we carried out ex vivo autoradiography in Tg2576 using [^{18}F]**21**, we obtained almost the same results as with [^{18}F]**10** (data not shown). The results suggest that these probes penetrated the blood−brain barrier and selectively labeled the Aβ plaques in the brain, as reflected by the biodistribution experiments and the in vitro binding assays.

Furthermore, we also investigated the effectiveness for neuropathological staining of Aβ plaques in human AD brain sections (Figure 5). A previous report suggested the configuration/folding of Aβ plaques in Tg2576 mice to be different from the tertiary/quaternary structure of Aβ plaques in AD brains.[44] Therefore, it is important to evaluate the affinity for Aβ plaques in human AD brains. [^{18}F]**10** clearly stained many Aβ plaques in AD brains. In contrast, no apparent staining was observed in normal adult brain sections. The labeling pattern was consistent with that observed by immunohistochemical labeling with an antibody specific to Aβ. The same results were observed in in vitro autoradiography using [^{18}F]**21** (data not shown). These results indicate that [^{18}F]**10** may be applicable for in vivo imaging of Aβ plaques in AD brains and deserves further investigation as a potential probe for the diagnosis of AD.

In conclusion, on the basis of previous results, we designed and synthesized two novel fluorinated pyridylbenzofuran and phenylbenzofuran ligands **10** and **21** for the imaging of Aβ plaques in the brain. These ligands showed high affinity for Aβ aggregates in vitro and for Aβ plaques in sections of autopsied AD brain. In biodistribution experiments using normal mice, they displayed good uptake into and fast washout from the brain, especially [^{18}F]**10**. In addition, ex vivo autoradiograms of brain sections from Tg2576 mice after the injection of [^{18}F]**10** showed selective binding of Aβ plaques with little nonspecific binding. The results suggest that [^{18}F]**10** should be further investigated as a potentially useful PET imaging agent for cerebral Aβ plaques. [^{18}F]**10** is currently in preparation for clinical trials.

EXPERIMENTAL SECTION

General Remarks. All chemicals used in syntheses were commercial products used without further purification. ^{1}H NMR spectra were obtained at 400 MHz on JEOL JNM-AL400 NMR spectrometers at room temperature with TMS as an internal standard. Chemical shifts are reported as δ values relative to the internal TMS. Coupling constants are reported in hertz. Multiplicity is defined by s (singlet), d (doublet), t (triplet), and m (multiplet). Mass spectra were acquired with a Shimadzu GC-MS-QP2010 Plus (ESI). HPLC was performed with a Shimadzu system (a LC-10AT pump with a SPD-10A UV detector, λ = 254 nm) with a Cosmosil C_{18} column (Nakalai Tesque, 5C_{18}-AR-II, 4.6 mm × 150 mm) using acetonitrile/water (60:40) as the mobile phase at a flow rate of 1.0 mL/min. Fluorescent observation was performed by microscope (Nikon Eclipse 80i) with a BV-2A filter set (excitation, 400−440 nm; diachronic mirror, 455 nm; long pass filter, 470 nm). All key compounds were proven to show ≥95% purity by HPLC.

Chemistry. 5-(5-Methoxy-2-benzofuranyl)-2-pyridinamine (1). A solution of 5-methoxybenzofuran-2-boronic acid (576 mg, 3.0 mmol), 2-amino-5-iodopyridine (660 mg, 3.0 mmol), and $(Ph_3)_4Pd$ (366 mg, 0.3 mmol) in 2 M Na_2CO_3/dioxane (150 mL, 1:1) was stirred under reflux overnight. After the mixture had cooled to room temperature, 1 M NaOH (20 mL) was added and extraction with ethyl acetate was carried out. The organic phase was dried over Na_2SO_4 and filtered. The filtrate was concentrated and the residue was purified by silica gel chromatography (hexane/ethyl acetate = 1:1) to give 374 mg of **1** (52.1%). ^{1}H NMR (400 MHz, $CDCl_3$): δ 3.85 (s, 3H), 4.67 (s, 2H), 6.59 (d, 1H, J = 8.8 Hz), 6.76 (s, 1H), 6.82 (dd, 1H, J_1= 8.8 Hz, J_2= 2.4 Hz), 7.07 (d, 1H, J = 2.4 Hz), 7.36 (d, 1H, J = 8.8 Hz), 7.86 (dd, 1H, J_1= 8.8 Hz, J_2= 2.4 Hz), 8.67 (d, 1H, J = 2.4 Hz). MS: m/z 241 (M^+ + H).

5-(5-Methoxy-2-benzofuranyl)-*N*-methyl-2-pyridinamine (2). Sodium methoxide (275 mg, 5.0 mmol) was added to **1** (240 mg, 1.0 mmol) in methanol (15 mL) followed by paraformaldehyde (101 mg, 4.0 mmol). The solution was heated to reflux for 2 h and cooled to 0 °C with an ice bath. Sodium borohydride (128 mg, 4.0 mmol) was added. The reaction mixture was brought to reflux again for 1 h and poured onto crushed ice. After a standard workup with ethyl acetate, the residue was purified by silica gel chromatography (hexane/ethyl acetate = 1:1) to give 234 mg of **2** (92.1%). ^{1}H NMR (400 MHz, $CDCl_3$): δ 2.98 (d, 3H, J = 5.2 Hz), 3.84 (s, 3H), 4.78 (s, 1H), 6.47 (d, 1H, J = 8.8 Hz), 6.76 (s, 1H), 6.84 (dd, 1H, J_1 = 8.8 Hz, J_2 = 4.4 Hz), 7.00 (d, 1H, J = 2.4 Hz), 7.36 (d, 1H, J = 8.4 Hz), 7.87 (dd, 1H, J_1 = 8.8 Hz, J_2 = 2.4 Hz), 8.59 (d, 1H, J = 2.8 Hz). MS: m/z 255 (M^+ + H).

2-(6-Methylamino-3-pyridinyl)-5-benzofuranol (3). BBr_3 (4.8 mL, 1 M solution in CH_2Cl_2) was added to a solution of **2** (234 mg, 0.92 mmol) in CH_2Cl_2 (20 mL) dropwise in an ice bath. The mixture was allowed to warm to room temperature and stirred for 1 h. Water (20 mL) was added while the reaction mixture was cooled in an ice bath. The mixture was extracted with ethyl acetate, and the organic phase was dried over Na_2SO_4 and filtered. The filtrate was concentrated, and the residue was purified by silica gel chromatography (hexane/ethyl acetate = 1:1) to give 218 mg of **3** (99.0%). ^{1}H NMR (400 MHz, $CDCl_3$): δ 2.98 (d, 3H, J = 5.2 Hz), 4.78 (s, 1H), 6.47 (d, 1H, J = 8.8 Hz), 6.76 (s, 1H), 6.84 (dd, 1H, J_1 = 8.8 Hz, J_2 = 4.4 Hz), 7.00 (d, 1H, J = 2.4 Hz), 7.36 (d, 1H, J = 8.4 Hz), 7.87 (dd, 1H, J_1 = 8.8 Hz, J_2 = 2.4 Hz), 8.59 (d, 1H, J = 2.8 Hz). MS: m/z 241 (M^+ + H).

2-(2-(2-(2-(6-(Methylamino)-3-pyridinyl)-5-benzofuranyloxy)ethoxy)ethoxy)ethanol (4). To a solution of **3** (197 mg, 0.82

dx.doi.org/10.1021/jm200057u |*J. Med. Chem.* 2011, 54, 2971–2979

mmol) and 2-[2-(2-chloroethoxy)ethoxy]ethanol (180 μL, 1.20 mmol) in DMF (5 mL) was added anhydrous K_2CO_3 (414 mg, 3.0 mmol). The reaction mixture was stirred for 18 h at 100 °C and then poured into water and extracted with chloroform. The organic layers were combined and dried over Na_2SO_4. Evaporation of the solvent afforded a residue, which was purified by silica gel chromatography (hexane/ethyl acetate = 1:6) to give 224 mg of **4** (60.3%). ^{1}H NMR (400 MHz, $CDCl_3$): δ 2.98 (d, 3H, J = 5.2 Hz), 3.62 (d, 2H, J = 4.4 Hz), 3.70−3.74 (m, 6H), 3.84 (s, 2H), 4.11 (s, 2H), 5.18 (s, 1H), 6.47 (d, 1H, J = 8.8 Hz), 6.76 (s, 1H), 6.84 (dd, 1H, J_1 = 8.8 Hz, J_2 = 4.4 Hz), 7.00 (d, 1H, J = 2.4 Hz), 7.36 (d, 1H, J = 8.4 Hz), 7.87 (dd, 1H, J_1 = 8.8 Hz, J_2 = 2.4 Hz), 8.59 (d, 1H, J = 2.8 Hz). MS: m/z 373 ($M^+ + H$).

5-(5-(2-(2-(2-(*tert*-Butyldimethylsilyloxy)ethoxy)ethoxy)-ethoxy)benzofuran-2-yl)-*N*-methylpyridin-2-amine (5). **4** (61 mg, 0.17 mmol) and TBDMSCl (41 mg, 0.27 mmol) were dissolved in dichloromethane (10 mL) followed by imidazole (24 mg, 0.34 mmol). The solution was stirred at room temperature for 2 h. After a standard workup with ethyl acetate, the residue was purified by silica gel chromatography (hexane/ethyl acetate = 1:6) to give 73 mg of **5** (87.6%). ^{1}H NMR (400 MHz, $CDCl_3$): δ 0.08 (s, 6H), 0.90 (s, 9H), 2.98 (d, 3H, J = 5.2 Hz), 3.62 (d, 2H, J = 4.4 Hz), 3.70−3.74 (m, 6H), 3.84 (s, 2H), 4.11 (s, 2H), 5.18 (s, 1H), 6.47 (d, 1H, J = 8.8 Hz), 6.76 (s, 1H), 6.84 (dd, 1H, J_1 = 8.8 Hz, J_2 = 4.4 Hz), 7.00 (d, 1H, J = 2.4 Hz), 7.36 (d, 1H, J = 8.4 Hz), 7.87 (dd, 1H, J_1 = 8.8 Hz, J_2 = 2.4 Hz), 8.59 (d, 1H, J = 2.8 Hz). MS: m/z 487 ($M^+ + H$).

***tert*-Butyl 5-(5-(2-(2-(2-(*tert*-Butyldimethylsilyloxy)ethoxy)ethoxy)-2-benzofuranyl)-2-pyridinyl-(methyl)carbamate (6).** **5** (73 mg, 0.15 mmol) was dissolved in anhydrous THF (5.0 mL) followed by Boc anhydride (66 mg, 0.30 mmol). The solution was refluxed overnight. After a standard workup with ethyl acetate, the residue was purified by silica gel chromatography (hexane/ethyl acetate = 1:1) to give 37 mg of **6** (46.7%). ^{1}H NMR (400 MHz, $CDCl_3$): δ 0.03 (s, 6H), 0.86 (s, 9H), 1.50 (s, 9H), 3.37 (s, 3H), 3.62−3.68 (m, 6H), 3.82−3.88 (m, 2H), 4.09−4.12 (m, 2H), 6.86 (d, 1H, J = 4.4 Hz), 6.88 (s, 1H), 6.98 (d, 1H, J = 2.4 Hz), 7.33 (d, 1H, J = 8.8 Hz), 7.76 (d, 1H, J = 10.0 Hz), 7.95 (dd, 1H, J_1 = 8.8 Hz, J_2 = 2.4 Hz), 8.75 (d, 1H, J = 1.6 Hz). MS: m/z 587 ($M^+ + H$).

***tert*-Butyl 5-(5-(2-(2-(2-Hydroxyethoxy)ethoxy)ethoxy)-2-benzofuranyl)-2-pyridinyl(methyl)carbamate (7).** TBAF (1 M in THF, 0.30 mL) was added via a syringe to a solution of **6** (37 mg, 0.07 mL) in THF (5 mL). The solution was stirred at room temperature for 5 h. After a standard workup with ethyl acetate, the residue was purified by silica gel chromatography (hexane/ethyl acetate = 1:1) to give 31 mg of **7** (93.0%). ^{1}H NMR (400 MHz, $CDCl_3$): δ 1.57 (s, 9H), 3.45 (s, 3H), 3.62−3.65 (m, 2H), 3.70−3.78 (m, 6H), 3.83−3.93 (m, 2H), 4.07−4.18 (m, 2H), 6.87(d, 1H, J = 6.8 Hz), 6.94 (s, 1H), 7.06 (d, 1H, J = 2.4 Hz), 7.40 (d, 1H, J = 9.2 Hz), 7.82 (d, 1H, J = 8.8 Hz), 8.02 (dd, 1H, J_1 = 8.8 Hz, J_2 = 2 Hz), 8.83 (d, 1H, J = 2.8 Hz). MS: m/z 473 ($M^+ + H$).

2-(2-(2-(2-(6-(*tert*-Butoxycarbonyl)-3-pyridinyl)-5-benzofuranyloxy)ethoxy)ethoxy)ethyl Methanesulfonate (8). **7** (30.5 mg, 0.065 mmol) was dissolved in dichloromethane (5 mL) followed by triethylamine (35 mg, 0.35 mmol). Methanesulfonyl chloride (25 mg, 0.21 mmol) was then added via a syringe. The solution was stirred at room temperature for 3 h. After a standard workup with ethyl acetate, the residue was purified by silica gel chromatography (hexane/ethyl acetate = 1:6) to give 25 mg of **8** (74.5%). ^{1}H NMR (400 MHz, $CDCl_3$): δ 1.54 (s, 9H), 3.06 (s, 3H), 3.44 (s, 3H), 3.69−3.72 (m, 6H), 3.79−3.88 (m, 2H), 4.11−4.17 (m, 2H), 4.37−4.39 (m, 2H), 6.90 (dd, 1H, J_1 = 9.2 Hz, J_2 = 2.8 Hz), 6.95 (s, 1H), 7.05 (d, 1H, J = 2.4 Hz), 7.40 (d, 1H, J = 8.8 Hz), 7.83 (d, 1H, J = 8.0 Hz), 8.02 (dd, 1H, J_1 = 8.8 Hz, J_2 = 2.4 Hz), 8.83 (d, 1H, J = 0.8 Hz). HRMS EI: m/z calcd for $C_{26}H_{34}N_2O_9S$ (M^+) 550.1985, found 550.1989.

***tert*-Butyl 5-(5-(2-(2-(2-Fluoroethoxy)ethoxy)ethoxy)-2-benzofuranyl)-2-pyridinyl(methyl)carbamate (9).** TBAF (1 M in THF, 0.20 mL) was added to a solution of **8** (27 mg, 0.05 mmol) in anhydrous THF (10 mL). The mixture was refluxed for 4 h. Afterward, it was cooled to room temperature. After a standard workup with ethyl acetate, the residue was purified by silica gel chromatography (hexane/ethyl acetate = 1:1) to give 22 mg of **9** (94.0%). ^{1}H NMR (400 MHz, $CDCl_3$): δ 1.57 (s, 9H), 3.44 (s, 3H), 3.71−3.83 (m, 6H), 3.88−3.91 (m, 2H), 4.22−4.51 (m, 1H), 4.61−4.63 (m, 1H), 6.91 (dd, 1H, J_1 = 8.8 Hz, J_2 = 2.4 Hz), 6.94 (s, 1H), 7.05 (d, 1H, J = 6.0 Hz), 7.38 (d, 1H, J = 8.8 Hz), 7.81 (d, 1H, J = 8.8 Hz), 8.02 (dd, 1H, J_1 = 8.8 Hz, J_2 = 2.4 Hz), 8.82 (d, 1H, J = 2.4 Hz). MS: m/z 475 ($M^+ + H$).

5-(5-(2-(2-(2-Fluoroethoxy)ethoxy)ethoxy)benzofuran-2-yl)-*N*-methylpyridin-2-amine (10). Trifluoroacetic acid (1.27 mL) was added slowly to a solution of **9** (22 mg, 0.047 mmol) in dichloromethane (2 mL). The mixture was then stirred at room temperature for 1 h. After a standard workup with ethyl acetate, the residue was purified by silica gel chromatography (hexane/ethyl acetate = 1:1) to give 9 mg of **10** (50.6%). ^{1}H NMR (400 MHz, $CDCl_3$): δ 2.98 (d, 3H, J = 5.2 Hz), 3.71−3.80 (m, 6H), 3.79−3.88 (m, 2H), 4.11−4.18 (m, 2H), 4.49−4.51 (m, 1H), 4.61−4.63 (m, 1H), 4.80 (s, 1H), 6.45 (d, 1H, J = 8.8 Hz), 6.75 (s, 1H), 6.85 (dd, 1H, J_1 = 8.8 Hz, J_2 = 2.4 Hz), 7.01 (d, 1H, J = 2.4 Hz), 7.36 (d, 1H, J = 9.2 Hz), 7.86 (dd, 1H, J_1 = 8.8 Hz, J_2 = 2.4 Hz), 8.59 (d, 1H, J = 2.0 Hz). HRMS (EI: m/z calcd for $C_{20}H_{23}FN_2O_4$ (M^+) 374.1642, found 374.1650.

5-Methoxy-2-(4-nitrophenyl)benzofuran (11). A solution of 2-hydroxy-5-methoxybenzaldehyde (1.22 g, 8.02 mmol), 4-nitrobenzyl bromide (1.73 g, 8.02 mmol), and K_2CO_3 (3.33 g, 24.06 mmol) in DMF (10 mL) was stirred under reflux overnight. The solvent was removed and the residue was recrystallized with ethyl acetate to give 1.39 g of **11** (64.0%). ^{1}H NMR (400 MHz, $CDCl_3$): δ 3.85 (s, 3H), 6.96−7.00 (m, 1H), 7.08 (d, 1H, J = 2.8 Hz), 7.18 (d, 1H, J = 2.8 Hz), 7.45 (d, 1H, J = 2.8 Hz), 7.95 (d, 2H, J = 8.8 Hz), 8.31 (d, 2H, J = 8.8 Hz).

5-Methoxy-2-(4-aminophenyl)benzofuran (12). A mixture of **11** (1.39 g, 5.16 mmol), $SnCl_2$ (5.82 g, 25.8 mmol), and ethanol (20 mL) was stirred under reflux for 2 h. After the mixture had cooled to room temperature, 1 M NaOH (20 mL) was added and extraction with ethyl acetate was carried out. The organic phase was dried over Na_2SO_4 and filtered. The filtrate was concentrated and the residue was purified by silica gel chromatography (hexane/ethyl acetate = 7:3) to give 609 mg of **12** (49.0%). ^{1}H NMR (400 MHz, $CDCl_3$): δ 3.85 (s, 3H), 6.71 (d, 2H, J = 8.8 Hz), 6.75 (s, 1H), 6.82 (dd, 1H, J_1 = 8.8 Hz, J_2 = 1.6 Hz), 6.97 (d, 1H, J = 2.8 Hz), 7.35 (d, 1H, J = 8.8 Hz), 7.65 (d, 2H, J = 8.8 Hz). MS: m/z 240 ($M^+ + H$).

5-Methoxy-2-(4-methylaminophenyl)benzofuran (13). A solution of NaOMe (5 M in MeOH, 4.0 mL) was added to a mixture of **12** (609 mg, 2.55 mmol) and paraformaldehyde (279 mg, 10.3 mmol) in methanol (30 mL) dropwise. The mixture was stirred under reflux for 1 h. After $NaBH_4$ (225 mg, 7.0 mmol) was added, the solution was heated under reflux for 2 h. Then 1 M NaOH (30 mL) was added to the cold mixture and extraction with $CHCl_3$ (30 mL) was conducted. The organic phase was dried over Na_2SO_4 and filtered. The solvent was removed, and the residue was purified by silica gel chromatography (hexane/ethyl acetate = 7:3) to give 616 mg of **13** (95.0%). ^{1}H NMR (400 MHz, $CDCl_3$): δ 2.84 (s, 3H), 3.85 (s, 3H), 6.71 (d, 2H, J = 8.8 Hz), 6.75 (s, 1H), 6.82 (dd, 1H, J_1 = 8.8 Hz, J_2 = 1.6 Hz), 6.97 (d, 1H, J = 2.8 Hz), 7.35 (d, 1H, J = 8.8 Hz), 7.65 (d, 2H, J = 8.8 Hz). MS: m/z 254 ($M^+ + H$).

5-Hydroxy-2-(4-methylaminophenyl)benzofuran (14). BBr_3 (12.4 mL, 1 M solution in CH_2Cl_2) was added to a solution of **13** (616 mg, 2.43 mmol) in CH_2Cl_2 (40 mL) dropwise in an ice bath. The mixture was allowed to warm to room temperature and stirred for 1 h. Water (20 mL) was added while the reaction mixture was cooled in an ice bath. The mixture was extracted with ethyl acetate, and the organic phase was dried over Na_2SO_4 and filtered. The filtrate was concentrated, and the residue was purified by silica gel chromatography (hexane/ethyl

acetate = 7:3) to give 576 mg of **14** (99.0%). ^{1}H NMR (400 MHz, $CDCl_3$): δ 2.92 (s, 3H), 3.92 (s, 1H), 6.64 (d, 2H, J = 8.4 Hz), 6.68 (s, 1H), 6.71 (dd, 1H, J_1 = 8.8 Hz, J_2 = 2.4 Hz), 6.93 (d, 1H, J = 2.4 Hz), 7.30 (d, 1H, J = 8.4 Hz), 7.70 (d, 2H, J = 8.4 Hz). MS: m/z 240 ($M^+ + H$).

2-(2-(2-(2-(4-(Methylamino)phenyl)benzofuran-5-yloxy)ethoxy)ethoxy)ethanol (15). To a solution of **14** (575 mg, 2.41 mmol) and 2-[2-(2-chloroethoxy)ethoxy]ethanol (810 μL, 8.91 mmol) in DMF (10 mL) was added anhydrous K_2CO_3 (1.23 g, 8.91 mmol). The reaction mixture was stirred for 18 h at 100 °C and then poured into water and extracted with chloroform. The organic layers were combined and dried over Na_2SO_4. Evaporation of the solvent afforded a residue, which was purified by silica gel chromatography (hexane/ethyl acetate = 1:6) to give 654 mg of **15** (73.2%). ^{1}H NMR (400 MHz, $CDCl_3$): δ 2.84 (s, 3H), 3.49−3.52 (m, 2H), 3.58−3.64 (m, 6H), 3.71−3.82 (m, 2H), 4.08−4.11 (m, 2H), 6.59 (d, 2H, J = 8.8 Hz), 6.65 (s, 1H), 6.77 (dd, 1H, J_1 = 8.8 Hz, J_2 = 2.8 Hz), 6.94 (d, 1H, J = 2.4 Hz), 7.26 (d, 1H, J = 8.8 Hz), 7.60 (d, 2H, J = 8.8 Hz). MS: m/z 486 ($M^+ + H$).

4-(5-(2-(2-(2-(*tert*-Butyldimethylsilyloxy)ethoxy)ethoxy)-ethoxy)benzofuran-2-yl)-*N*-methylbenzenamine (16). **15** (383 mg, 1.03 mmol) and TBDMSCl (243 mg, 1.61 mmol) were dissolved in dichloromethane (10 mL) followed by imidazole (142 mg, 2.06 mmol). The solution was stirred at room temperature for 4 h. After a standard workup with ethyl acetate, the residue was purified by silica gel chromatography (hexane/ethyl acetate = 1:1) to give 453 mg of **16** (90.6%). ^{1}H NMR (400 MHz, $CDCl_3$): δ 0.02 (s, 6H), 0.83 (s, 9H), 2.84 (s, 3H), 3.49−3.52 (m, 2H), 3.58−3.64 (m, 6H), 3.71−3.82 (m, 2H), 4.08−4.11 (m, 2H), 6.59 (d, 2H, J = 8.8 Hz), 6.65 (s, 1H), 6.77 (dd, 1H, J_1 = 8.8 Hz, J_2 = 2.8 Hz), 6.94 (d, 1H, J = 2.4 Hz), 7.26 (d, 1H, J = 8.8 Hz), 7.60 (d, 2H, J = 8.8 Hz). MS: m/z 486 ($M^+ + H$).

***tert*-Butyl 4-(5-(2-(2-(2-(*tert*-Butyldimethylsilyloxy)ethoxy)ethoxy)benzofuran-2-yl)phenyl-(methyl)carbamate (17).** Compound **16** (452 mg, 0.93 mmol) was dissolved in anhydrous THF (20 mL) followed by Boc anhydride (601 mg, 1.79 mmol). The solution was refluxed overnight. After standard workup with ethyl acetate, the residue was purified by silica gel chromatography (hexane/ethyl acetate = 7:3) to give 412 mg of **17** (75.6%). ^{1}H NMR (400 MHz, $CDCl_3$): δ 0.02 (s, 6H), 0.83 (s, 9H), 3.20 (s, 3H), 3.47−3.52 (m, 2H), 3.59−3.67 (m, 6H), 3.71−3.82 (m, 2H), 4.08−4.11 (m, 2H), 6.82 (d, 2H, J = 8.4 Hz), 6.95 (d, 1H, J = 3.6 Hz), 7.23 (d, 2H, J = 8.8 Hz), 7.29 (d, 1H, J = 8.4 Hz), 7.70 (d, 2H, J = 8.8 Hz). MS: m/z 586 ($M^+ + H$).

***tert*-Butyl 4-(5-(2-(2-(2-Hydroxyethoxy)ethoxy)ethoxy)-benzofuran-2-yl)phenyl(methyl)carbamate (18).** TBAF (1 M in THF, 1.83 mL) was added via a syringe to a solution of **17** (412 mg, 0.70 mL) in THF (10 mL). The solution was stirred at room temperature for 2 h. After a standard workup with ethyl acetate, the residue was purified by silica gel chromatography (hexane/ethyl acetate = 1:1) to give 324 mg of **18** (97.9%). ^{1}H NMR (400 MHz, $CDCl_3$): δ 1.40 (s, 9H), 3.18 (s, 3H), 3.49−3.53 (m, 2H), 3.58−3.66 (m, 6H), 3.74−3.79 (m, 2H), 6.82 (d, 2H, J = 8.4 Hz), 6.95 (d, 1H, J = 3.6 Hz), 7.22 (d, 2H, J = 8.8 Hz), 7.29 (d, 1H, J = 8.4 Hz), 7.70 (d, 2H, J = 8.8 Hz). MS: m/z 472 ($M^+ + H$).

2-(2-(2-(2-(4-(*tert*-Butoxycarbonyl)phenyl)benzofuran-5-yloxy)ethoxy)ethoxy)ethyl Methanesulfonate (19). **18** (324 mg, 0.688 mmol) was dissolved in dichloromethane (20 mL) followed by triethylamine (344 mg, 3.44 mmol). Methanesulfonyl chloride (237 mg, 2.06 mmol) was then added via a syringe. The solution was stirred at room temperature for 2 h. After a standard workup with ethyl acetate, the residue was purified by silica gel chromatography (hexane/ethyl acetate = 1:1) to give 374 mg of **19** (98.8%). ^{1}H NMR (400 MHz, $CDCl_3$): δ 1.47 (s, 9H), 3.02 (s, 3H), 3.26 (s, 3H), 3.63−3.72 (m, 6H), 3.79−3.82 (m, 2H), 4.32−4.35 (m, 2H), 6.86 (dd, 1H, J_1 = 8.8 Hz, J_2 = 2.4 Hz), 6.90 (s, 1H), 7.02 (d, 1H, J = 2.8 Hz), 7.30 (d, 2H, J = 8.8 Hz), 7.36 (d, 1H, J = 8.4 Hz), 7.76 (d, 2H, J = 8.8 Hz). HRMS EI: m/z calcd for $C_{27}H_{35}NO_9S$ (M^+) 549.6331, found 549.2025.

***tert*-Butyl 4-(5-(2-(2-(2-Fluoroethoxy)ethoxy)ethoxy)benzofuran-2-yl)phenyl(methyl)carbamate (20).** TBAF (1 M in THF, 0.50 mL) was added to a solution of **20** (55.3 mg, 0.10 mmol) in anhydrous THF (5 mL). The mixture was refluxed for 2 h and cooled to room temperature. After a standard workup with ethyl acetate, the residue was purified by silica gel chromatography (hexane/ethyl acetate = 1:1) to give 46 mg of **20** (97.2%). ^{1}H NMR (400 MHz, $CDCl_3$): δ 1.47 (s, 9H), 3.29 (s, 3H), 3.70−3.73 (m, 6H), 3.78−3.80 (m, 2H), 4.15−4.18 (m, 2H), 4.48−4.62 (m, 2H), 6.89−6.92 (m, 2H), 7.04 (d, 1H, J = 2.8 Hz), 7.30 (d, 2H, J = 8.8 Hz), 7.37 (d, 1H, J = 5.2 Hz), 7.79 (d, 2H, J = 8.8 Hz). MS: m/z 474 ($M^+ + H$).

4-(5-(2-(2-(2-Fluoroethoxy)ethoxy)ethoxy)benzofuran-2-yl)-*N*-methylbenzenamine (21). Trifluoroacetic acid (2.70 mL) was added slowly to a solution of **20** (46.0 mg, 0.10 mmol) in dichloromethane (3 mL). The mixture was then stirred at room temperature for 1 h. After a standard workup with ethyl acetate, the residue was purified by silica gel chromatography (hexane/ethyl acetate = 1:1) to give 16 mg of **21** (43.4%). ^{1}H NMR (400 MHz, $CDCl_3$): δ 2.88 (s, 3H), 3.72−3.75 (m, 6H), 3.87−3.89 (m, 2H), 4.05−4.11 (m, 2H), 4.49−4.63 (m, 2H), 6.65 (d, 2H, J = 8.8 Hz), 6.71 (s, 1H), 6.82 (dd, 1H, J_1 = 8.8 Hz, J_2 = 2.8 Hz), 7.00 (d, 1H, J = 2.4 Hz), 7.33 (d, 1H, J = 8.8 Hz), 7.66 (d, 2H, J = 8.8 Hz). HRMS EI: m/z calcd for $C_{21}H_{24}FNO_4$ (M^+) 373.4180, found 373.1683.

Binding Assays Using the Aggregated Aβ Peptides in Solution. Aβ(1−42) was purchased from Peptide Institute (Osaka, Japan). Aggregation was carried out by gently dissolving the peptide (0.25 mg/mL) in a buffer solution (pH 7.4) containing 10 mM sodium phosphate and 1 mM EDTA. The solution was incubated at 37 °C for 42 h with gentle and constant shaking. A mixture containing 50 μL of test compounds (0.008 pM to 400 μM in 10% EtOH), 50 μL of 0.02 nM [^{125}I]IMPY, 50 μL of Aβ(1−42) aggregates, and 850 μL of 10% EtOH was incubated at room temperature for 3 h. The mixture was then filtered through Whatman GF/B filters using a Brandel M-24 cell harvester, and the radioactivity of the filters containing the bound ^{125}I ligand was measured in a γ counter. Values for the half maximal inhibitory concentration (IC_{50}) were determined from displacement curves of three independent experiments using GraphPad Prism 5.0, and those for the inhibition constant (K_i) were calculated using the Cheng−Prusoff equation:[45] $K_i = IC_{50}/(1 + [L]/K_d)$, where [L] is the concentration of [^{125}I]IMPY used in the assay and K_d is the dissociation constant of IMPY (4.2 nM).

Radiolabeling with ^{18}F. [^{18}F]Fluoride was produced by cyclotron (CYPRIS HM-18, Sumitomo Heavy Industries, Tokyo) via an ^{18}O (p, n)^{18}F reaction and passed through a Sep-Pak Light QMA cartridge (Waters) as an aqueous solution in ^{18}O-enriched water. The cartridge was dried by N_2, and the ^{18}F activity was eluted with 1.0 mL of a Kryptofix 222/K_2CO_3 solution (9.5 mg of Kryptofix 222 and 1.7 mg of K_2CO_3 in acetonitrile/water (96/4)). The solvent was removed at 120 °C under a stream of argon gas. The residue was azeotropically dried with 1 mL of anhydrous acetonitrile twice at 120 °C under a stream of nitrogen gas. A solution of the mesylate precursors **8** and **19** (1.0 mg) in acetonitrile (200 μL) was added to the reaction vessel containing the ^{18}F activity. The mixture was heated at 120 °C for 5 min and was cooled for 1 min. HCl (10% aqueous solution, 450 μL) was then added, and the mixture was heated at 120 °C again for 5 min. An aqueous solution of NaOH was added to adjust the pH to 8−9. The mixture was extracted with ethyl acetate (1 mL × 2), and the solvent was removed under nitrogen gas. The residue was purified by preparative HPLC [YMC-Pack Pro C_{18} column (20 mm × 150 mm), acetonitrile/water (70/30), flow rate of 4.0 mL/min]. The retention time of the desired ^{18}F-labeled product is 13.3 min. The radiochemical purity and specific activity were determined by analytical HPLC [YMC-Pack Pro C_{18} column (4.6 mm × 150 mm), acetonitrile/water (50/50), flow rate of 1.0 mL/min], and [^{18}F]**10** and [^{18}F]**21** were obtained in a radiochemical purity of >99%

with a specific activity of 242 GBq/μmol. Specific activity was estimated by comparing the UV peak intensity of the purified ^{18}F-labeled compound with a reference nonradioactive compound of known concentration.

Biodistribution in Normal Mice. Experiments with animals were conducted in accordance with our institutional guidelines and approved by the Kyoto University Animal Care Committee. While under anesthesia with isoflurane, ddY mice (22−25 g, male) were injected directly into the tail vein with 100 μL of a 0.1% BSA solution containing [^{18}F]**10** and [^{18}F]**21** (185−370 kBq). The mice (n = 5 for each time point) were sacrificed at 2, 10, 30, and 60 min postinjection. The organs of interest were removed and weighed, and radioactivity was measured with an automatic γ counter (COBRAII, Packard). Percentage dose per organ was calculated by a comparison of the tissue counts to suitably diluted aliquots of the injected material. The % dose/g of samples was calculated by comparing the sample counts with the count of the diluted initial dose.

In Vitro Autoradiography Using Brain Sections from AD Patients. Post-mortem brain sections (5 μm, temporal lobe) of an AD patient and a control subject (5 μm, temporal lobe) were obtained from BioChain Institute Inc. They were incubated with [^{18}F]**10** and [^{18}F]**21** (444 kBq/50 μL) for 1 h at room temperature. The sections were then dipped in saturated Li_2CO_3 in 40% EtOH (two 2-min washes), washed with 40% EtOH (one 2-min wash), and rinsed with water for 30 s. After drying, the ^{18}F-labeled sections were exposed to a BAS imaging plate (Fuji Film, Tokyo, Japan) overnight. Autoradiographic images were obtained using a BAS5000 scanner system (Fuji Film).

Ex Vivo Autoradiography Using Tg2576 Mice. Tg2576 transgenic mice (36 months, male) and wild-type mice (36 months, male) were purchased from Taconic Farms, Inc. and used as an Alzheimer's model and an age-matched control, respectively. After anesthetization with 1% isoflurane, 11.1 MBq [^{18}F]**10** or [^{18}F]**21** in 200 μL of 0.1% BSA solution was injected through a tail vein. The animals were allowed to recover for 30 min and then killed by decapitation. The brains were immediately removed and frozen in dry ice/hexane bath. Sections of 20 μm were cut and exposed to a BAS imaging plate (Fuji Film, Tokyo, Japan) overnight. Ex vivo film autoradiograms were thus obtained. After autoradiographic examination, the same sections were stained by thioflavin-S to confirm the presence of Aβ plaques. For the staining of thioflavin-S, sections were immersed in a 0.125% thioflavin-S solution containing 50% EtOH for 3 min and washed in 50% EtOH. After drying, the sections were then examined using a microscope (Nikon, Eclipse 80i) equipped with a B-2A filter set (excitation, 450−490 nm; diachronic mirror, 505 nm; long-pass filter, 520 nm).

■ ASSOCIATED CONTENT

Supporting Information. Preparation for ^{18}F-labeling of **10** and **21**. This material is available free of charge via the Internet at http://pubs.acs.org.

■ AUTHOR INFORMATION

Corresponding Author

*For M.O.: phone, +81-75-753-4608; fax, +81-75-753-4568; e-mail, ono@pharm.kyoto-u.ac.jp. For H.S.: phone, +81-75-753-4556; fax, +81-75-753-4568, e-mail, hsaji@pharm.kyoto-u.ac.jp.

■ ACKNOWLEDGMENT

The study was supported by the Funding Program for Next Generation World-Leading Researchers and a Grant-in-Aid for Young Scientists (A) and Exploratory Research from the Ministry of Education, Culture, Sports, Science and Technology, Japan.

■ ABBREVIATIONS USED

AD, Alzheimer's disease; Aβ, β-amyloid; NFT, neurofibrillary tangle; PET, positron emission tomography; SB-13, 4-*N*-methylamino-4′-hydroxystilbene; PIB, 2-(4′-(methylaminophenyl)-6-hydroxybenzothiazole; FDDNP, 2-(1-(2-(*N*-(2-fluoroethyl)-*N*-methylamino)naphthalene-6-yl)ethylidene)malononitrile; FPHBF-1, 4-(5-(2-(2-(2-fluoroethoxy)ethoxy)ethoxy)benzofuran-2-yl)-*N*,*N*-dimethylbenzenamine; FPYBF-1, 5-(5-(2-(2-(2-fluoroethoxy)ethoxy)ethoxy)benzofuran-2-yl)-*N*,*N*-dimethylpyridin-2-amine; TBAF, tetra-*n*-butylammonium fluoride; THF, tetrahydrofuran; BOC, *tert*-butyloxycarbonyl; TBDMSCl, *tert*-butyldimethylsilyl chloride; IMPY, 2-(4′-dimethylaminophenyl)-6-iodoimidazo[1,2-*a*]pyridine

■ REFERENCES

(1) Hardy, J. A.; Higgins, G. A. Alzheimer's disease: the amyloid cascade hypothesis. *Science* **1992**, *256*, 184–185.

(2) Selkoe, D. J. Alzheimer's disease: genes, proteins, and therapy. *Physiol. Rev.* **2001**, *81*, 741–766.

(3) Selkoe, D. J. Imaging Alzheimer's amyloid. *Nat. Biotechnol.* **2000**, *18*, 823–824.

(4) Mathis, C. A.; Wang, Y.; Klunk, W. E. Imaging β-amyloid plaques and neurofibrillary tangles in the aging human brain. *Curr. Pharm. Des.* **2004**, *10*, 1469–1492.

(5) Nordberg, A. PET imaging of amyloid in Alzheimer's disease. *Lancet Neurol.* **2004**, *3*, 519–527.

(6) Ono, M.; Wilson, A.; Nobrega, J.; Westaway, D.; Verhoeff, P.; Zhuang, Z. P.; Kung, M. P.; Kung, H. F. ^{11}C-labeled stilbene derivatives as Aβ-aggregate-specific PET imaging agents for Alzheimer's disease. *Nucl. Med. Biol.* **2003**, *30*, 565–571.

(7) Verhoeff, N. P.; Wilson, A. A.; Takeshita, S.; Trop, L.; Hussey, D.; Singh, K.; Kung, H. F.; Kung, M. P.; Houle, S. In-vivo imaging of Alzheimer disease β-amyloid with [^{11}C]SB-13 PET. *Am. J. Geriatr. Psychiatry* **2004**, *12*, 584–595.

(8) Mathis, C. A.; Wang, Y.; Holt, D. P.; Huang, G. F.; Debnath, M. L.; Klunk, W. E. Synthesis and evaluation of ^{11}C-labeled 6-substituted 2-arylbenzothiazoles as amyloid imaging agents. *J. Med. Chem.* **2003**, *46*, 2740–2754.

(9) Klunk, W. E.; Engler, H.; Nordberg, A.; Wang, Y.; Blomqvist, G.; Holt, D. P.; Bergstrom, M.; Savitcheva, I.; Huang, G. F.; Estrada, S.; Ausen, B.; Debnath, M. L.; Barletta, J.; Price, J. C.; Sandell, J.; Lopresti, B. J.; Wall, A.; Koivisto, P.; Antoni, G.; Mathis, C. A.; Langstrom, B. Imaging brain amyloid in Alzheimer's disease with Pittsburgh compound-B. *Ann. Neurol.* **2004**, *55*, 306–319.

(10) Kudo, Y.; Okamura, N.; Furumoto, S.; Tashiro, M.; Furukawa, K.; Maruyama, M.; Itoh, M.; Iwata, R.; Yanai, K.; Arai, H. 2-(2-[2-Dimethylaminothiazol-5-yl]ethenyl)-6-(2-[fluoro]ethoxy)benzoxazole: a novel PET agent for in vivo detection of dense amyloid plaques in Alzheimer's disease patients. *J. Nucl. Med.* **2007**, *48*, 553–561.

(11) Johnson, A. E.; Jeppsson, F.; Sandell, J.; Wensbo, D.; Neelissen, J. A.; Jureus, A.; Strom, P.; Norman, H.; Farde, L.; Svensson, S. P. AZD2184: a radioligand for sensitive detection of β-amyloid deposits. *J. Neurochem.* **2009**, *108*, 1177–1186.

(12) Swahn, B. M.; Wensbo, D.; Sandell, J.; Sohn, D.; Slivo, C.; Pyring, D.; Malmstrom, J.; Arzel, E.; Vallin, M.; Bergh, M.; Jeppsson, F.; Johnson, A. E.; Jureus, A.; Neelissen, J.; Svensson, S. Synthesis and evaluation of 2-pyridylbenzothiazole, 2-pyridylbenzoxazole and 2-pyridylbenzofuran derivatives as ^{11}C-PET imaging agents for β-amyloid plaques. *Bioorg. Med. Chem. Lett.* **2010**, *20*, 1976–1980.

(13) Agdeppa, E. D.; Kepe, V.; Liu, J.; Flores-Torres, S.; Satyamurthy, N.; Petric, A.; Cole, G. M.; Small, G. W.; Huang, S. C.; Barrio, J. R. Binding characteristics of radiofluorinated 6-dialkylamino-2-naphthylethylidene derivatives as positron emission tomography imaging probes for β-amyloid plaques in Alzheimer's disease. *J. Neurosci.* **2001**, *21*, RC189.

(14) Shoghi-Jadid, K.; Small, G. W.; Agdeppa, E. D.; Kepe, V.; Ercoli, L. M.; Siddarth, P.; Read, S.; Satyamurthy, N.; Petric, A.; Huang, S. C.; Barrio, J. R. Localization of neurofibrillary tangles and β-amyloid plaques in the brains of living patients with Alzheimer disease. *Am. J. Geriatr. Psychiatry* **2002**, *10*, 24–35.

(15) Koole, M.; Lewis, D. M.; Buckley, C.; Nelissen, N.; Vandenbulcke, M.; Brooks, D. J.; Vandenberghe, R.; Van Laere, K. Whole-body biodistribution and radiation dosimetry of ^{18}F-GE067: a radioligand for in vivo brain amyloid imaging. *J. Nucl. Med.* **2009**, *50*, 818–822.

(16) Vandenberghe, R.; Van Laere, K.; Ivanoiu, A.; Salmon, E.; Bastin, C.; Triau, E.; Hasselbalch, S.; Law, I.; Andersen, A.; Korner, A.; Minthon, L.; Garraux, G.; Nelissen, N.; Bormans, G.; Buckley, C.; Owenius, R.; Thurfjell, L.; Farrar, G.; Brooks, D. J. ^{18}F-Flutemetamol amyloid imaging in Alzheimer disease and mild cognitive impairment: a phase 2 trial. *Ann. Neurol.* **2010**, *68*, 319–329.

(17) Nelissen, N.; Van Laere, K.; Thurfjell, L.; Owenius, R.; Vandenbulcke, M.; Koole, M.; Bormans, G.; Brooks, D. J.; Vandenberghe, R. Phase 1 study of the Pittsburgh compound B derivative ^{18}F-flutemetamol in healthy volunteers and patients with probable Alzheimer disease. *J. Nucl. Med.* **2009**, *50*, 1251–1259.

(18) Zhang, W.; Oya, S.; Kung, M. P.; Hou, C.; Maier, D. L.; Kung, H. F. F-18 polyethyleneglycol stilbenes as PET imaging agents targeting Aβ aggregates in the brain. *Nucl. Med. Biol.* **2005**, *32*, 799–809.

(19) Rowe, C. C.; Ackerman, U.; Browne, W.; Mulligan, R.; Pike, K. L.; O'Keefe, G.; Tochon-Danguy, H.; Chan, G.; Berlangieri, S. U.; Jones, G.; Dickinson-Rowe, K. L.; Kung, H. P.; Zhang, W.; Kung, M. P.; Skovronsky, D.; Dyrks, T.; Holl, G.; Krause, S.; Friebe, M.; Lehman, L.; Lindemann, S.; Dinkelborg, L. M.; Masters, C. L.; Villemagne, V. L. Imaging of amyloid β in Alzheimer's disease with ^{18}F-BAY94-9172, a novel PET tracer: proof of mechanism. *Lancet Neurol.* **2008**, *7*, 129–135.

(20) O'Keefe, G. J.; Saunder, T. H.; Ng, S.; Ackerman, U.; Tochon-Danguy, H. J.; Chan, J. G.; Gong, S.; Dyrks, T.; Lindemann, S.; Holl, G.; Dinkelborg, L.; Villemagne, V.; Rowe, C. C. Radiation dosimetry of β-amyloid tracers ^{11}C-PiB and ^{18}F-BAY94-9172. *J. Nucl. Med.* **2009**, *50*, 309–315.

(21) Zhang, W.; Kung, M. P.; Oya, S.; Hou, C.; Kung, H. F. ^{18}F-Labeled styrylpyridines as PET agents for amyloid plaque imaging. *Nucl. Med. Biol.* **2007**, *34*, 89–97.

(22) Choi, S. R.; Golding, G.; Zhuang, Z.; Zhang, W.; Lim, N.; Hefti, F.; Benedum, T. E.; Kilbourn, M. R.; Skovronsky, D.; Kung, H. F. Preclinical properties of ^{18}F-AV-45: a PET agent for Aβ plaques in the brain. *J. Nucl. Med.* **2009**, *50*, 1887–1894.

(23) Wong, D. F.; Rosenberg, P. B.; Zhou, Y.; Kumar, A.; Raymont, V.; Ravert, H. T.; Dannals, R. F.; Nandi, A.; Brasic, J. R.; Ye, W.; Hilton, J.; Lyketsos, C.; Kung, H. F.; Joshi, A. D.; Skovronsky, D. M.; Pontecorvo, M. J. In vivo imaging of amyloid deposition in Alzheimer disease using the radioligand ^{18}F-AV-45 (flobetapir F 18). *J. Nucl. Med.* **2010**, *51*, 913–920.

(24) Liu, Y.; Zhu, L.; Plossl, K.; Choi, S. R.; Qiao, H.; Sun, X.; Li, S.; Zha, Z.; Kung, H. F. Optimization of automated radiosynthesis of [^{18}F]AV-45: a new PET imaging agent for Alzheimer's disease. *Appl. Radiat. Isot.* **2010**, *68*, 2293–2297.

(25) Lin, K. J.; Hsu, W. C.; Hsiao, I. T.; Wey, S. P.; Jin, L. W.; Skovronsky, D.; Wai, Y. Y.; Chang, H. P.; Lo, C. W.; Yao, C. H.; Yen, T. C.; Kung, M. P. Whole-body biodistribution and brain PET imaging with [^{18}F]AV-45, a novel amyloid imaging agent—a pilot study. *Nucl. Med. Biol.* **2010**, *37*, 497–508.

(26) Clark, C. M.; Schneider, J. A.; Bedell, B. J.; Beach, T. G.; Bilker, W. B.; Mintun, M. A.; Pontecorvo, M. J.; Hefti, F.; Carpenter, A. P.; Flitter, M. L.; Krautkramer, M. J.; Kung, H. F.; Coleman, R. E.; Doraiswamy, P. M.; Fleisher, A. S.; Sabbagh, M. N.; Sadowsky, C. H.; Reiman, P. E.; Zehntner, S. P.; Skovronsky, D. M. Use of florbetapir-PET for imaging β-amyloid pathology. *J. Am. Med. Assoc.* **2011**, *305*, 275–283.

(27) Kung, H. F.; Choi, S. R.; Qu, W.; Zhang, W.; Skovronsky, D. ^{18}F stilbenes and styrylpyridines for PET imaging of Aβ plaques in Alzheimer's disease: a miniperspective. *J. Med. Chem.* **2010**, *53*, 933–941.

(28) Ono, M.; Kung, M. P.; Hou, C.; Kung, H. F. Benzofuran derivatives as Aβ-aggregate-specific imaging agents for Alzheimer's disease. *Nucl. Med. Biol.* **2002**, *29*, 633–642.

(29) Ono, M.; Kawashima, H.; Nonaka, A.; Kawai, T.; Haratake, M.; Mori, H.; Kung, M. P.; Kung, H. F.; Saji, H.; Nakayama, M. Novel benzofuran derivatives for PET imaging of β-amyloid plaques in Alzheimer's disease brains. *J. Med. Chem.* **2006**, *49*, 2725–2730.

(30) Cheng, Y.; Ono, M.; Kimura, H.; Kagawa, S.; Nishii, R.; Kawashima, H.; Saji, H. Fluorinated benzofuran derivatives for PET imaging of β-amyloid plaques in Alzheimer's disease brains. *ACS Med. Chem. Lett.* **2010**, *1*, 321–325.

(31) Ono, M.; Yoshida, N.; Ishibashi, K.; Haratake, M.; Arano, Y.; Mori, H.; Nakayama, M. Radioiodinated flavones for in vivo imaging of β-amyloid plaques in the brain. *J. Med. Chem.* **2005**, *48*, 7253–7260.

(32) Ono, M.; Haratake, M.; Mori, H.; Nakayama, M. Novel chalcones as probes for in vivo imaging of β-amyloid plaques in Alzheimer's brains. *Bioorg. Med. Chem.* **2007**, *15*, 6802–6809.

(33) Cheng, Y.; Ono, M.; Kimura, H.; Kagawa, S.; Nishii, R.; Saji, H. A novel ^{18}F-labeled pyridyl benzofuran derivative for imaging of β-amyloid plaques in Alzheimer's brains. *Bioorg. Med. Chem. Lett.* **2010**, *20*, 6141–6144.

(34) Miyaura, N.; Yamada, K.; Suzuki, A. A new stereospecific cross-coupling by the palladium-catalyzed reaction of 1-alkenylboranes with 1-alkenyl or 1-alkynyl halides. *Tetrahedron Lett.* **1979**, *36*, 3437–3440.

(35) Ono, M.; Haratake, M.; Saji, H.; Nakayama, M. Development of novel β-amyloid probes based on 3,5-diphenyl-1,2,4-oxadiazole. *Bioorg. Med. Chem.* **2008**, *16*, 6867–6872.

(36) Watanabe, H.; Ono, M.; Ikeoka, R.; Haratake, M.; Saji, H.; Nakayama, M. Synthesis and biological evaluation of radioiodinated 2,5-diphenyl-1,3,4-oxadiazoles for detecting β-amyloid plaques in the brain. *Bioorg. Med. Chem.* **2009**, *17*, 6402–6406.

(37) Kung, H. F.; Lee, C. W.; Zhuang, Z. P.; Kung, M. P.; Hou, C.; Plossl, K. Novel stilbenes as probes for amyloid plaques. *J. Am. Chem. Soc.* **2001**, *123*, 12740–12741.

(38) Ono, M.; Haratake, M.; Nakayama, M.; Kaneko, Y.; Kawabata, K.; Mori, H.; Kung, M. P.; Kung, H. F. Synthesis and biological evaluation of (*E*)-3-styrylpyridine derivatives as amyloid imaging agents for Alzheimer's disease. *Nucl. Med. Biol.* **2005**, *32*, 329–335.

(39) Ono, M.; Watanabe, R.; Kawashima, H.; Cheng, Y.; Kimura, H.; Watanabe, H.; Haratake, M.; Saji, H.; Nakayama, M. Fluoro-pegylated chalcones as positron emission tomography probes for in vivo imaging of β-amyloid plaques in Alzheimer's disease. *J. Med. Chem.* **2009**, *52*, 6394–6401.

(40) Maya, Y.; Ono, M.; Watanabe, H.; Haratake, M.; Saji, H.; Nakayama, M. Novel radioiodinated aurones as probes for SPECT imaging of β-amyloid plaques in the brain. *Bioconjugate Chem.* **2009**, *20*, 95–101.

(41) Hsiao, K.; Chapman, P.; Nilsen, S.; Eckman, C.; Harigaya, Y.; Younkin, S.; Yang, F.; Cole, G. Correlative memory deficits, Aβ elevation, and amyloid plaques in transgenic mice. *Science* **1996**, *274*, 99–102.

(42) Ono, M.; Hayashi, S.; Kimura, H.; Kawashima, H.; Nakayama, M.; Saji, H. Push−pull benzothiazole derivatives as probes for detecting β-amyloid plaques in Alzheimer's brains. *Bioorg. Med. Chem.* **2009**, *17*, 7002–7007.

(43) Ono, M.; Watanabe, R.; Kawashima, H.; Kawai, T.; Watanabe, H.; Haratake, M.; Saji, H.; Nakayama, M. ^{18}F-Labeled flavones for in vivo imaging of β-amyloid plaques in Alzheimer's brains. *Bioorg. Med. Chem.* **2009**, *17*, 2069–2076.

(44) Toyama, H.; Ye, D.; Ichise, M.; Liow, J. S.; Cai, L.; Jacobowitz, D.; Musachio, J. L.; Hong, J.; Crescenzo, M.; Tipre, D.; Lu, J. Q.; Zoghbi, S.; Vines, D. C.; Seidel, J.; Katada, K.; Green, M. V.; Pike, V. W.; Cohen, R. M.; Innis, R. B. PET imaging of brain with the β-amyloid probe, [^{11}C]6-OH-BTA-1, in a transgenic mouse model of Alzheimer's disease. *Eur. J. Nucl. Med. Mol. Imaging* **2005**, *32*, 593–600.

(45) Cheng, Y.; Prusoff, W. Relationship between the inhibition constant (K1) and the concentration of inhibitor which causes 50% inhibition (I50) of an enzymatic reaction. *Biochem. Pharmacol.* **1973**, *22*, 3099–3108.

(46) Leo, A. J. Calculating log P_{oct} from structures. *Chem. Rev.* **1993**, *93*, 1281–1306.